SOILS AND FOUNDATIONS Vol. 48, No. 3, 419–432, June 2008
Japanese Geotechnical Society

FORMULATION OF A DUSTY GAS MODEL FOR MULTI-COMPONENT DIFFUSION IN THE GAS PHASE OF SOIL

YOSHIHIKO HIBI[i)]

ABSTRACT

Soil vapor extraction and bio-venting have been utilized for purification of contaminated soil or groundwater. It is necessary to predict the movement of gas phase components in soil for the design of soil vapor extraction and bio-venting systems. Though chemical substances migrate with advection and diffusion in gas phase of soil, we investigated multi-component diffusion systems in gas phase of soil. Numerical modeling for multi-component diffusion is useful to the prediction of the movement of components. A dusty gas model for multi-component diffusion systems has not so far been formulated by the Finite Element Method; furthermore it has not been applied for assessing the movement of components in the gas phase of soil. Accordingly, a dusty gas model for three gas phase components was formulated by the Finite Element Method in this study, and the concentrations of components in binary and multi-component gas systems were calculated by numerical methods developed in this study. As a result, it was found that the dusty gas model must be applied for study of diffusion in a multi-component gas system; and the study showed that the difference between molecular weights of gas phase components influenced the movement of components in the gas system.

Key words: dusty gas model, finite element method, multi-component diffusion, numerical analysis, unsaturated soil (**IGC**: E13)

INTRODUCTION

Soil vapor extraction and bio-venting have been used to purify contaminated soil and groundwater (Shan and Javandel, 1992). In soil vapor extraction, gas phase soil components are extracted by a vacuum pump and harmful gases are adsorbed onto activated carbon. In bio-venting, oxygen is pumped into the soil to support the growth of microbes which break down the organic liquid contaminants present in the soil. In these cases, the gas phases present in the soil (oxygen, nitrogen, harmful gas, etc) disperse and advect in a multi-component gas system. It is important to predict the migration of components in the gas phase by a numerical model. The prediction of gas migration by numerical modeling is useful to the design of soil vapor extraction and bio-venting systems.

Previous studies (Abriola and Pinder, 1985; Sleep and Skyes, 1993) have developed a numerical model with multiphase flow, gas flow, and advective-dispersion transport of components in the vapor zone. Fick's law was formulated in that model for dispersion of components in the vapor zone. Moreover, Lenhard et al. (1995), Kneafsey and Hunt (2004), Jellali et al. (2003), Mendoza and Frind (1990), Mendoza and Frind (1990), Sleep and Sykes (1989), Corapcioglu and Baeh (1987), Costanza-Robinson, and Brusseau (2002), Baehr and Corapcioglu (1987) have simulated the migration of trichloroethylene or hexane gas in a binary gas system composed of air and these gases by numerical models applying Fick's law. Fick's law can be applied for diffusion in a binary gas system, and is represented by

$$\mathbf{N}_i = -D_{ij}\nabla c_i \tag{1}$$

where $\mathbf{N}_i$ is the molar flux [mol/L^{2}T] of component i in a binary gas system, D_{ij} is a binary molecular diffusion coefficient [L^2/T] between component i and component j, and c_i is the molar concentration [mol/L^3] of component i. Actually the components in the gas phase of soil may diffuse in a multi-component gas system in most cases, but there are a few cases in which the components diffuse in a binary gas system. The application of Fick's law is restricted to systems that exhibit binary gas diffusion. Advection of chemical components is significantly in the multi-component gas system and has been solved for mass transfer in groundwater. However, multi-component diffusion in gas phase of soil has not been investigated except for Fick's law. Accordingly, we investigate multi-component diffusion in this study.

A diffusion coefficient which considers molecular diffusion in a multi-component gas system can be employed in place of the binary diffusion coefficient in Eq. (1) as long as each component is present in low concentrations. In this case, the molecular diffusion coefficient can be given by Blanc's law (Poling et al., 2001) if the concentration of

[i)] Department of Environmental Science and Technology, Faculty of Science and Technology, Meijo University, Nagoya, Japan (hibiy@ccmfs.meijo-u.ac.jp).
The manuscript for this paper was received for review on August 27, 2007; approved on February 5, 2008.
Written discussions on this paper should be submitted before January 1, 2009 to the Japanese Geotechnical Society, 4-38-2, Sengoku, Bunkyo-ku, Tokyo 112-0011, Japan. Upon request the closing date may be extended one month.

each component is very low.

$$D_{\mathrm{im}} = \frac{1}{\sum_{J=1}^{n} \frac{X_{\mathrm{j}}}{D_{\mathrm{ij}}}} \tag{2}$$

In the equation, D_{im} is a molecular diffusion coefficient [L^2/T] in the multi-component gas system, X_{j} is the molar fraction [dimensionless] of component j, and n is the number of components. Hoeg et al. (2004) simulated the migration of low concentration gas phase 1,1,1 trichloroethane, 1,1,2 trichloroethane, and trichloroethylene in soil by a numerical model applying Eqs. (1) and (2). The results of the simulation were compared with results of experiments carried out by Fischer et al. (1996), and it was demonstrated that the results of simulation were consistent with experimental results.

Poling et al. (2001) indicated that Eq. (2) was derived from Stefan-Maxwell equations (Curtiss and Hirschfelder, 1949) as follows:

$$\sum_{\substack{J=1 \\ J \neq i}}^{n} \frac{X_{\mathrm{i}}\mathbf{N}_{\mathrm{j}} - X_{\mathrm{j}}\mathbf{N}_{\mathrm{i}}}{D_{\mathrm{ij}}} = \nabla c_{\mathrm{i}} \tag{3}$$

Equation (3) represents the diffusion of components in multi-component systems with accuracy, and can be applied to molecular diffusion in multi-component gas systems even if the concentration of each component is high. The diffusion in Eq. (3) occurs when molecules collide with each other, as shown in Fig. 1.

Baehr and Bruell (1990) carried out experiments on the advective-diffusion of hexane, benzene, and isooctane in oxygen and nitrogen gas systems in the vertical direction. The concentrations of the organic species were predicted by Fick's law or the Stefan-Maxwell equations, assuming that the molar flux of oxygen approaches zero over time. It was found by comparison between the predicted concentration and the concentration observed in the advective-diffusion experiments that the concentration predicted by Fick's law was similar to the concentration given by the Stefan-Maxwell equations. Massmann and Farrier (1992) reported similar results by demonstrating fluxes of trichloroethylene in oxygen and nitrogen gas systems which were calculated by multi-component equations or a single-component equation derived from Fick's law. The multi-component equations (called ''dusty gas'' model equations) were derived from the Stefan-Maxwell equations with Knudsen diffusion flux and viscous flux. Knudsen diffusion occurs when molecules collide with surfaces of soil particles, as shown in Fig. 1. Massmann and Farrier (1992) concluded that it was possible to apply a Fick's law-type equation when the permeability is more than 10^{-10} cm^2.

The above mentioned results were derived for conditions of restricted permeability, or where some of the molar fluxes in Eq. (3) were zero, i.e., when the flux of some components was stagnant. However, Eq. (3) cannot be solved for the molar fraction or concentration and the molar flux of each component unless it is assumed that some molar flux is zero, or has a defined relationship to another molar flux.

Therefore it is not suitable to apply Fick's law Eq. (1) to multi-component gas systems, suggesting the use of the dusty gas model equations. On the other hand, the dusty gas model equations have never been completely formulated with either the Finite Element Method (FEM) or the Fine Difference Method (FDM). This study attempts to solve the dusty gas model equations by FEM, and several different gas systems will be simulated by the numerical model developed in this study. The results will demonstrate the difference between the diffusion coefficient calculated by Eq. (2) and the diffusion coefficient calculated by the dusty gas model in a binary gas system, and the difference between the concentration simulated by the numerical model using Eqs. (2) and (1) and the concentration simulated by the numerical model developed in this study.

NECESSITY FOR THE DUSTY GAS MODEL

Mason (1967) and Mason and Malinauskas (1983) derived multi-component diffusion equations with diffusion flux and viscous flux depending on temperature from a dusty gas model, and Cunningham and Williams (1980) explained the process of induction for Stefan-Maxwell equations and multi-component diffusion equations, adding a term for the Knudsen diffusion to the Stefan-Maxwell equations. Knudsen diffusion is a phenomenon wherein molecules of gas diffuse by colliding with the sur-

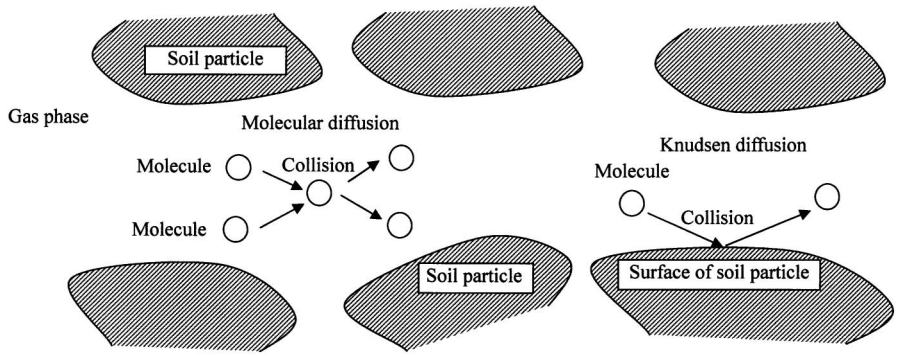

Fig. 1. Schemata of Molecular diffusion and Knudsen diffusion

faces of soil particles. Reinecke and Sleep (2002) demonstrated a relationship between the Knudsen coefficient, soil permeability, and the Klinkenberg parameter (Klinkenberg, 1941), and Thostenson and Pollock (1989) investigated the influence of Knudsen diffusion flux on multi-component diffusion in the soil gas phase.

The dusty gas model equation without viscous flux under constant temperature is,

$$\sum_{\substack{i=1\\ i\neq j}}^{n} \frac{X_i\mathbf{N}_j - X_j\mathbf{N}_i}{D_{ij}} - \frac{\mathbf{N}_j}{D_i} = \nabla c_j \tag{4}$$

where D_i is the Knudsen coefficient [L^2/T], and the secondary term of the left side indicates Knudsen diffusion.

A Comparison between an Equation based on Fick's Law and an Equation Derived by the Dusty Gas Model

The dusty gas model for a binary gas system can be expressed for components A and B as follows.
Component A

$$\frac{X_A\mathbf{N}_B - X_B\mathbf{N}_A}{D_{AB}} - \frac{\mathbf{N}_A}{D_A} = \nabla c_A \tag{5a}$$

Component B

$$\frac{X_B\mathbf{N}_A - X_A\mathbf{N}_B}{D_{AB}} - \frac{\mathbf{N}_B}{D_B} = \nabla c_B \tag{5b}$$

In these equations, X_A and X_B are molar fractions [dimensionless] of component A and component B, $\mathbf{N}_B$ and $\mathbf{N}_A$ are molar fluxes [mol/L^2T] of components A and B, and c_A are c_B molar concentrations of components A and B [mol/L^3], D_{AB} is the molecular diffusivity [L^2/T] of component A in component B or B in A, and D_A and D_B are the Knudsen diffusivities [L^2/T] of components A and B, respectively.

On other hand, the following equation may be derived by Graham's law (Cunningham and Williams, 1980) for binary system when the total gas pressure is constant in an analytical domain.

$$\mathbf{N}_A M_A^{1/2} + \mathbf{N}_B M_B^{1/2} = 0 \tag{6}$$

where M_A and M_B are the molecular weights [M/mol] of component A and component B, respectively.

By substituting Eqs. (6) into (5) and re-arranging, $\mathbf{N}_A$ and $\mathbf{N}_B$ can be obtained as follows,

$$\mathbf{N}_A = -\frac{\nabla c_A}{\frac{X_A}{D_{AB}}\left(\frac{M_A}{M_B}\right)^{1/2} + \frac{X_B}{D_{AB}} + \frac{1}{D_A}} \tag{7a}$$

$$\mathbf{N}_B = -\frac{\nabla c_B}{\frac{X_B}{D_{AB}}\left(\frac{M_B}{M_A}\right)^{1/2} + \frac{X_A}{D_{AB}} + \frac{1}{D_B}} \tag{7b}$$

By comparison between Eqs. (1) and (7), molecular diffusion coefficients in Eq. (1) correspond with the D^*_{AB} and D^*_{BA} defined from Eq. (7). Because particles of soil resist molecular diffusion in the soil gas phase, the molecular diffusion coefficient with soil particles present in the system is generally smaller than the molecular diffusion coefficient without soil particles (Millington, 1959). The D^*_{AB} and D^*_{BA} take account of tortuosity τ [dimensionless], which influences the paths of components in the soil gas phase.

$$D^*_{AB} = \frac{1}{\frac{X_A}{\tau D_{AB}}\left(\frac{M_A}{M_B}\right)^{1/2} + \frac{X_B}{\tau D_{AB}} + \frac{1}{D_A}} \tag{8a}$$

$$D^*_{BA} = \frac{1}{\frac{X_B}{\tau D_{AB}}\left(\frac{M_B}{M_A}\right)^{1/2} + \frac{X_A}{\tau D_{AB}} + \frac{1}{D_B}} \tag{8b}$$

A molecular diffusion equation in the form of Fick's law taking account of tortuosity can be expressed for the molar flux of component A as follows:

$$N_A = -\tau D_{AB}\nabla c_A \tag{9}$$

Furthermore, a molecular diffusion coefficient taking account of tortuosity for component A approximates Eq. (10) when the component is present at low concentration.

$$D^*_{AB} = \frac{1}{\frac{X_B}{\tau D_{AB}} + \frac{1}{D_A}} \tag{10}$$

Equation (8a) without a Knudsen diffusion coefficient is consistent with the binary diffusion coefficient of Eq. (9) if the molecular weight of component A is equal to the molecular weight of component B. Then, assuming that the concentration of component A is very low, X_B approximates 1.0. As a result, Eq. (10) without a Knudsen diffusion coefficient is almost equal to the binary diffusion coefficient of Eq. (9). If X_B is below 1.0 and Knudsen diffusion is taken account of, Eq. (10) is inconsistent with the binary diffusion coefficient of Eq. (9).

Therefore Eq. (10) has the limitation when the equation is applied to the binary diffusion coefficient. On the other hand Eq. (8a) can be applied for every situation encountered in a binary gas system without the limitation. The above mentioned conditions for application of Eqs. (8), (9) and (10) are arranged in Table 1.

A Comparison with Molecular Diffusion Coefficients in the Binary Gas System

Molecular diffusion coefficients have been calculated by Eqs. (8a) and (10), and the results are illustrated in Figs. 2 and 3. Chemical and physical parameters used in these calculations are indicated in Table 2.

The binary diffusion coefficient in Eq. (9) has been

Table 1. A comparison between conditions for application of each model

Model	Equation	Conditions for application
Dusty Gas Model	(8)	Without any restriction. In all cases for multi-component gas system.
Fick's law	(9)	In binary gas system.
Blanc's law	(10)	In cases that concentration of the diffusing gas is dilute.

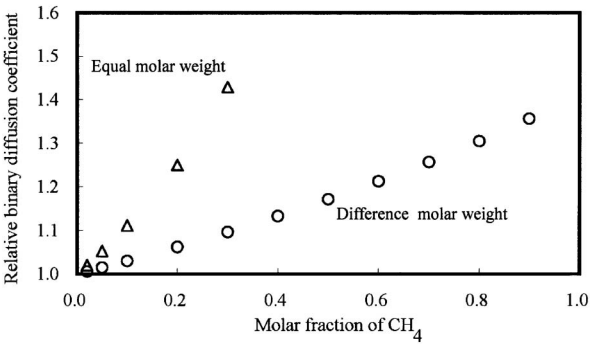

Fig. 2. Diffusion coefficients for binary gas system consisting of methane gas and air in the gas phase of soil. Circles in case of a difference between molecular weights, and triangles in case of equal molecular weights

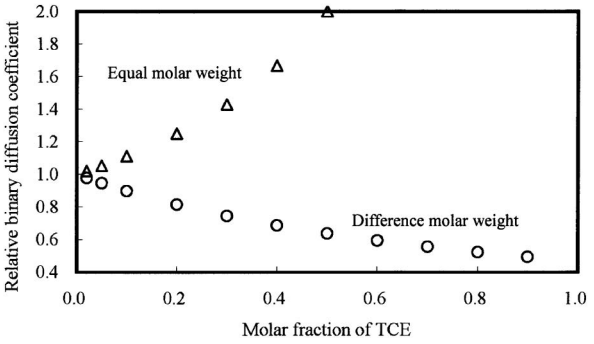

Fig. 3. Diffusion coefficients for binary gas system consisting of trichloroethylene and air in the gas phase of soil. Circles in case of a difference between molecular weights, and triangles in case of equal molecular weights

Table 2. Parameters for calculation of molecular diffusion coefficients for binary gas system

Parameter	Value and/or Units
Tortuosity, τ	0.1
Component A : air Molecular weight, M_A	28.75 g/mol
Component B: methane Molecular weight, M_B	16.04 g/mol
TCE Molecular weight, M_B	131.4 g/mol
Molecular diffusion coefficient between air and methane, D_{AB}	2.2×10^{-1} cm^2/s
Molecular diffusion coefficient between air and TCE, D_{AB}	7.6×10^{-2} cm^2/s

compared with the diffusion coefficient calculated by Eq. (8a) or Eq. (10) in a binary diffusion system consisting of air and methane. This situation implies that methane, of lower density than air, infiltrates through the air-gas system by molecular diffusion. Figure 2 shows the relationship between the molar fraction of methane in an air-methane system and the relative diffusion coefficient which divides the diffusion coefficient of Eq. (8a) or Eq. (10) by the diffusion coefficient of Eq. (9).

Relative diffusion coefficients calculated by Eq. (8a) or Eq. (10) exceed 1.0, and increase with the molar fraction of methane as shown in Fig. 2. It is found by a comparison between the molecular diffusion coefficients calculated by Eqs. (8a) and (10) that the relative diffusion coefficient given by Eq. (10) is larger than that given by Eq. (8a). Actually, the relative diffusion coefficient given by Eq. (10) should become 1.0 for the case of a molecular diffusion coefficient in a binary gas system without Knudsen diffusion and a difference in the molecular weight. The relative diffusion coefficient given by Eq. (10) becomes 1.02 as shown in Fig. 2 when the molar fraction of methane is 0.02 and 1.05 when the molar fraction of methane is 0.05. Therefore, Eq. (2) can be applied only where the molar fraction of methane is relatively low. The molecular diffusion coefficient given by Eq. (10) is not equal to the binary molecular diffusion coefficient for high concentrations of methane. Equation (10) must not be employed under conditions of high concentration components diffusing in a gas system. The molecular diffusion coefficient given by Eq. (8a) or Eq. (8b) should be equal to the diffusion coefficient in Eq. (9) if the molecular weight of component A is consistent with that of component B and Knudsen diffusion does not occur in gas system. The diffusion coefficient given by Eq. (8a) differs from the diffusion coefficient in Eq. (9) by reason of the $(X_A/\tau D_{AB})(M_A/M_B)^{1/2}$ term included in the numerator of Eq. (8a). The relative diffusion coefficient given by Eq. (8a) as shown in Fig. 2 becomes 1.03 when the molar fraction of methane is 0.05 and 1.06 when it is 0.10. Therefore the molecular diffusion coefficient is highly influenced by the difference in the molecular weight, and the binary diffusion coefficient of Eq. (9) can not be used when simulating a system of gases that are of significantly different molecular weights.

Figure 3 shows the relationship between the molar fraction of trichloroethylene (TCE) and a relative diffusion coefficient obtained by Eq. (8a) or Eq. (10) in a binary gas system consisting of air and TCE. The molecular weight of TCE is heavier than that of air, as shown in Table 2. The relative diffusion coefficient calculated by Eq. (10) is more than 1.0, similar to the case of the methane-in-air system, and Eq. (10) can be used for simulations of the molecular diffusion only if the concentration of TCE is sufficiently low. On the other hand, the relative diffusion coefficient calculated by Eq. (8a) does not exceed 1.0, and decreases with increasing TCE molar fraction. The relative diffusion coefficient given by Eq. (8a) is 0.95 as shown in Fig. 3 when the molar fraction of TCE is 0.05, and 0.90 when TCE molar fraction is 0.10. The diffusion coefficient given by Eq. (8a) may become smaller than that in Eq. (9) if the molecular weight of the gas diffusing into the system is heavier than that of the majority gas.

It was found in this investigation that Eq. (10) can be used for simulations of the molecular diffusion only if the concentration of gas diffusing into the system is very dilute, and that Eqs. (8a) and (8b) must be used for simulations of systems with gas phase components that differ in molecular weight. The total molar diffusion flux $\mathbf{N}^T$ is defined as the sum of the molar diffusion gas flux $\mathbf{N}^D$ [mol/L ^{2}T], given by Eq. (9) representing Fick's law, and a none-

quimolar diffusion gas flux $\mathbf{N}^T$ [mol/L^{2}T] (Thorstenson and Pollock, 1989, Cunnigham and William, 1980), which occurs by reason of the difference in gas molecular weight. The difference between the diffusion coefficients given by Eq. (8a) and the binary diffusion coefficient in Eq. (9) is a reason for the nonequimolar diffusion.

FORMULATION OF MOLECULAR DIFFUSION EQUATIONS FOA A THREE-COMPONENT GAS SYSTEM IN THE GAS PHASE OF SOIL

It was found in the binary gas system that a difference between molecular weights is very important, and Eq. (10) must be used when the concentration of the components diffusing into the gas system is very low. Then migrations of three components in a three-gas system in the soil gas phase will be simulated by the dusty gas model and Fick's law with Eq. (9). The results reported here make it clear that the dusty gas model is very significant for multi-component diffusion in soil gas phases.

The dusty gas model for three components can be expressed as follows.

Component A

$$\frac{X_A\mathbf{N}_B - X_B\mathbf{N}_A}{\tau D_{AB}} + \frac{X_A\mathbf{N}_C - X_C\mathbf{N}_A}{\tau D_{AC}} - \frac{\mathbf{N}_A}{D_A} = \nabla c_A \tag{11a}$$

Component B

$$\frac{X_B\mathbf{N}_A - X_A\mathbf{N}_B}{\tau D_{AB}} + \frac{X_B\mathbf{N}_C - X_C\mathbf{N}_B}{\tau D_{BC}} - \frac{\mathbf{N}_B}{D_B} = \nabla c_B \tag{11b}$$

Component C

$$\frac{X_C\mathbf{N}_A - X_A\mathbf{N}_C}{\tau D_{AC}} + \frac{X_C\mathbf{N}_B - X_B\mathbf{N}_C}{\tau D_{BC}} - \frac{\mathbf{N}_C}{D_C} = \nabla c_C \tag{11c}$$

In these equations, X_C is a molar fraction [dimensionless] of component C, $\mathbf{N}_C$ is a molar flux [mol/L^{2}T] of component C, c_C is a molar concentration of component C [mol/L^3], D_{BC} is a binary molecular diffusion coefficient [L^2/T] of component B in component C or C in B, D_{AC} is a binary molecular diffusion coefficient [L^2/T] of component A in component C or C in A and D_C is the Knudsen diffusion coefficient [L^2/T] of component C, respectively.

The equation of Graham's law for three components can be expressed as follows.

$$\mathbf{N}_A M_A^{1/2} + \mathbf{N}_B M_B^{1/2} + \mathbf{N}_C M_C^{1/2} = 0 \tag{12}$$

Arranging (11), $\mathbf{N}_A$, $\mathbf{N}_B$ and $\mathbf{N}_C$ can be given as the following equation.

$$\mathbf{N}_A = -\frac{\nabla c_A}{\left(\frac{X_B}{\tau D_{AB}} + \frac{X_C}{\tau D_{AC}} + \frac{1}{D_A}\right)} + \frac{X_A}{\tau D_{AB}\left(\frac{X_B}{\tau D_{AB}} + \frac{X_C}{\tau D_{AC}} + \frac{1}{D_A}\right)}\mathbf{N}_B + \frac{X_A}{\tau D_{AC}\left(\frac{X_B}{\tau D_{AB}} + \frac{X_C}{\tau D_{AC}} + \frac{1}{D_A}\right)}\mathbf{N}_C \tag{13a}$$

$$\mathbf{N}_B = -\frac{\nabla c_B}{\left(\frac{X_A}{\tau D_{AB}} + \frac{X_C}{\tau D_{BC}} + \frac{1}{D_B}\right)} + \frac{X_B}{\tau D_{AB}\left(\frac{X_A}{\tau D_{AB}} + \frac{X_C}{\tau D_{BC}} + \frac{1}{D_B}\right)}\mathbf{N}_A + \frac{X_B}{\tau D_{BC}\left(\frac{X_A}{\tau D_{AB}} + \frac{X_C}{\tau D_{BC}} + \frac{1}{D_B}\right)}\mathbf{N}_C \tag{13b}$$

$$\mathbf{N}_C = -\frac{\nabla c_C}{\left(\frac{X_A}{\tau D_{AC}} + \frac{X_B}{\tau D_{BC}} + \frac{1}{D_C}\right)} + \frac{X_C}{\tau D_{AC}\left(\frac{X_A}{\tau D_{AC}} + \frac{X_B}{\tau D_{BC}} + \frac{1}{D_C}\right)}\mathbf{N}_A + \frac{X_C}{\tau D_{BC}\left(\frac{X_A}{\tau D_{AC}} + \frac{X_B}{\tau D_{BC}} + \frac{1}{D_C}\right)}\mathbf{N}_B \tag{13c}$$

where D_A^*, D_B^*, and D_C^* in Eq. (13) are defined as follows:

$$D_A^* = \frac{1}{\left(\frac{X_B}{\tau D_{AB}} + \frac{X_C}{\tau D_{AC}} + \frac{1}{D_A}\right)} \tag{14a}$$

$$D_B^* = \frac{1}{\left(\frac{X_A}{\tau D_{AB}} + \frac{X_C}{\tau D_{BC}} + \frac{1}{D_B}\right)} \tag{14b}$$

$$D_C^* = \frac{1}{\left(\frac{X_A}{\tau D_{AC}} + \frac{X_B}{\tau D_{BC}} + \frac{1}{D_C}\right)} \tag{14c}$$

Substituting Eqs. (13) and (14) into equations of the conservation of mass law for each gas phase component of soil, the constituted equations Eq. (15) for each component in the soil gas phase can be induced as follows:

$$\theta_g \frac{\partial c_A}{\partial t} = \nabla\cdot(D_A^*\nabla c_A) - \nabla\cdot\left(\frac{D_A^* X_A}{\tau D_{AB}}\mathbf{N}_B\right) - \nabla\cdot\left(\frac{D_A^* X_A}{\tau D_{AC}}\mathbf{N}_C\right) \tag{15a}$$

$$\theta_g \frac{\partial c_B}{\partial t} = \nabla\cdot(D_B^*\nabla c_B) - \nabla\cdot\left(\frac{D_B^* X_B}{\tau D_{AB}}\mathbf{N}_A\right) - \nabla\cdot\left(\frac{D_B^* X_B}{\tau D_{BC}}\mathbf{N}_C\right) \tag{15b}$$

$$\theta_g \frac{\partial c_C}{\partial t} = \nabla\cdot(D_C^*\nabla c_C) - \nabla\cdot\left(\frac{D_C^* X_C}{\tau D_{AC}}\mathbf{N}_A\right) - \nabla\cdot\left(\frac{D_C^* X_C}{\tau D_{BC}}\mathbf{N}_B\right) \tag{15c}$$

where θ_g is the gas-filled porosity.

A differential equation like Eq. (15) can generally be solved approximately by means of the Finite Element Method (FEM) or Finite Difference method (FDM). FEM has an advantage that any shape of element can be used for discretization of the analytical domain. On the other

hand, quadrilateral elements except for the rectangle cannot be used in FDM, and rectangular elements are generally employed in FDM. FDM is superior to FEM for tracking the mass balance between that of a component injected into or discharged out of the analytical domain and changes of mass of a component in the analytical domain. However the Lumping method verified by Milly (1985) or Celia (1990) is able to improve mass balance which is calculated from the concentration of the component given by means of FEM, and the accuracy of the mass balance obtained by means of FEM with the Lumping method is as precise as that obtained by means of FDM. Therefore the Galerkin Finite Element Method (GFEM) is applied to solve Eq. (15) in this study, and if Φ_i is a basic function at node i for discretization of the analytical domain, each variable in Eq. (15) may be approximated by Φ_i as follows.

$$\theta_g = \sum_{i=1}^{np} \Phi_i \theta_{g_i} \tag{16a}$$

$$c_k = \sum_{i=1}^{np} \Phi_i c_{k_i} \quad \text{for } k = \text{Component A, B, C} \tag{16b}$$

$$D_k^* = \sum_{i=1}^{np} \Phi_i D_{k_i}^* \quad \text{for } k = \text{Component A, B, C} \tag{16c}$$

$$X_k = \sum_{i=1}^{np} \Phi_i X_{k_i} \quad \text{for } k = \text{Component A, B, C} \tag{16d}$$

$$\mathbf{N}_k = \sum_{i=1}^{np} \Phi_i \mathbf{N}_{k_i}^* \quad \text{for } k = \text{Component A, B, C} \tag{16e}$$

In these equations, a subscript i is the nodal number given at a node in the discrete domain, and the variables with subscript i are the physical or chemical values at each nodal number. Then np is the number of nodes.

When GFEM and Green's integral theorem are applied to Eq. (15), a weight function is equal to the basic function. Furthermore the time terms in Eq. (15) can be made discrete by the implicit Euler method, and the Picard iteration method is employed for linearization of the approximate equations of Eq. (15) because these equations are nonlinear in molar fractions of the components. As a result, the approximate equations of Eq. (15) with the Lumping method can be obtained as follows.

$$\begin{aligned}
&\frac{1}{\Delta t}\int_V \bar{\theta}_g^{t+\Delta t,m}\Phi_i dV c_{Ai}^{t+\Delta t,m+1} + \sum_{j=1}^{np}\int_V \bar{D}_A^{*\,t+\Delta t,m}\nabla\Phi_i\cdot\nabla\Phi_j dV c_{Aj}^{t+\Delta t,m+1} \\
&\quad = \frac{1}{\Delta t}\int_V \bar{\theta}_g^{t+\Delta t,m}\Phi_i dV c_{Ai}^{t} + \sum_{j=1}^{np}\int_V \frac{\bar{D}_A^{*\,t+\Delta t,m}\bar{X}^{t+\Delta t,m}}{D_{AB}}\nabla\Phi_i\cdot\Phi_j dV \mathbf{N}_{Bj}^{t+\Delta t,m} \\
&\quad\quad + \sum_{j=1}^{np}\int_V \frac{\bar{D}_A^{*\,t+\Delta t,m}\bar{X}_A^{t+\Delta t,m}}{D_{AC}}\nabla\Phi_i\cdot\Phi_i dV \mathbf{N}_{Cj}^{t+\Delta t,m} + \int_\Omega \Phi_i \mathbf{q}_A^{t+\Delta t}\cdot\mathbf{n}d\Omega \quad \text{for} \quad i = 1\sim np
\end{aligned} \tag{17a}$$

$$\begin{aligned}
&\frac{1}{\Delta t}\int_V \bar{\theta}_g^{t+\Delta t,m}\Phi_i dV c_{Bi}^{t+\Delta t,m+1} + \sum_{j=1}^{np}\int_V \bar{D}_B^{*\,t+\Delta t,m}\nabla\Phi_i\cdot\nabla\Phi_j dV c_{Bj}^{t+\Delta t,m+1} \\
&\quad = \frac{1}{\Delta t}\int_V \bar{\theta}_g^{t+\Delta t,m}\Phi_i dV c_{Bi}^{t} + \sum_{j=1}^{np}\int_V \frac{\bar{D}_B^{*\,t+\Delta t,m}\bar{X}_B^{t+\Delta t,m}}{D_{AB}}\nabla\Phi_i\cdot\Phi_j dV \mathbf{N}_{Aj}^{t+\Delta t,m} \\
&\quad\quad + \sum_{j=1}^{np}\int_V \frac{\bar{D}_B^{*\,t+\Delta t,m}\bar{X}_B^{t+\Delta t,m}}{D_{BC}}\nabla\Phi_i\cdot\Phi_j dV \mathbf{N}_{Cj}^{t+\Delta t,m} + \int_\Omega \Phi_i \mathbf{q}_B^{t+\Delta t}\cdot\mathbf{n}d\Omega \quad \text{for} \quad i = 1\sim np
\end{aligned} \tag{17b}$$

$$\begin{aligned}
&\frac{1}{\Delta t}\int_V \bar{\theta}_g^{t+\Delta t,m}\Phi_i dV c_{Ci}^{t+\Delta t,m+1} + \sum_{j=1}^{np}\int_V \bar{D}_C^{*t+\Delta t,m}\nabla\Phi_i\cdot\nabla\Phi_j dV c_{Cj}^{t+\Delta t,m+1} \\
&\quad = \frac{1}{\Delta t}\int_V \bar{\theta}_g^{t+\Delta t,m}\Phi_i dV c_{Ci}^{t} + \sum_{j=1}^{np}\int_V \frac{\bar{D}_C^{*t+\Delta t,m}\bar{X}_C^{t+\Delta t,m}}{D_{AC}}\nabla\Phi_i\cdot\Phi_j dV \mathbf{N}_{Aj}^{t+\Delta t,m} \\
&\quad\quad + \sum_{j=1}^{np}\int_V \frac{\bar{D}_C^{*t+\Delta t,m}\bar{X}_C^{t+\Delta t,m}}{D_{BC}}\nabla\Phi_i\cdot\Phi_j dV \mathbf{N}_{Bj}^{t+\Delta t,m} + \int_\Omega \Phi_i \mathbf{q}_C^{t+\Delta t}\cdot\mathbf{n}d\Omega \quad \text{for} \quad i = 1\sim np
\end{aligned} \tag{17c}$$

In the foregoing, unknown variable become $\mathbf{N}_A$, $\mathbf{N}_B$, $\mathbf{N}_C$, c_A, c_B and c_C, and superscripts t or $t+\Delta t$ indicate a time step in which time t elapses or time is incremented by Δt, and m or $m+1$ is an iteration number of the Picard iteration method. The terms $\bar{\theta}_g$, $\bar{D}_A^*$, $\bar{D}_B^*$, $\bar{D}_C^*$, $\bar{X}_A$, $\bar{X}_B$ and $\bar{X}_C$ are averages of the respective values of θ_g, D_A^*, D_B^*, D_C^*, X_A, X_B and X_C within each element, V is the whole volume [L^3] of the analytical domain, and Ω is a boundary of the analytical domain. Furthermore, $\mathbf{n}$ is normal vector to boundary Ω. The terms $\mathbf{q}_A$, $\mathbf{q}_B$, and $\mathbf{q}_C$ are molar fluxes [mol/L^2T] of components A, B, and C at the boundaries, respectively, and are defined as follows:

$$\mathbf{q}_A = D_A^*\nabla c_A - \frac{D_A^* X_A}{\tau D_{AB}}\mathbf{N}_B - \frac{D_A^* X_A}{\tau D_{AC}}\mathbf{N}_C \tag{18a}$$

$$\mathbf{q}_B = D_B^*\nabla c_B - \frac{D_B^* X_B}{\tau D_{AB}}\mathbf{N}_A - \frac{D_B^* X_B}{\tau D_{BC}}\mathbf{N}_C \tag{18b}$$

$$\mathbf{q}_C = D_C^*\nabla c_C - \frac{D_C^* X_C}{\tau D_{AC}}\mathbf{N}_A - \frac{D_C^* X_C}{\tau D_{BC}}\mathbf{N}_B \tag{18c}$$

The coefficients D_A^*, D_B^*, and D_C^* can be calculated from

molar fractions X_A, X_B and X_C, and each molar fraction can be divided by the concentration of each component as follows.

$$X_k = c_k/c, \text{ for } k = \text{component A, B, C} \tag{19}$$

where c is the total concentration ($= c_A + c_B + c_C$) [mol/L^3] in the analytical domain. Accordingly D_A^*, D_B^*, D_C^*, X_A, X_B and X_C can be obtained from the concentration of each component. It is necessary to assign $\mathbf{N}_A$, $\mathbf{N}_B$, $\mathbf{N}_C$ for the solutions of Eq. (17) because there are more unknown variables than the number of the constituted equations. Therefore $\mathbf{N}_A$, $\mathbf{N}_B$ and $\mathbf{N}_C$ in Eq. (17) is given from a previous iteration step by mean of Picard iteration method. These variables must be obtained from the latest concentrations of the components in the Picard iteration step. Values of $\mathbf{N}_A$, $\mathbf{N}_B$ and $\mathbf{N}_C$ may be obtained by Eqs. (11) and (12).

By substituting Eq. (12) into Eq. (11b) and re-arranging, Eq. (20) can be obtained as follows:

$$\left\{\left(\frac{(M_B/M_A)^{1/2}}{\tau D_{AB}} - \frac{1}{\tau D_{BC}}\right)X_B + \left(\frac{1}{\tau D_{AB}} - \frac{1}{\tau D_{BC}}\right)X_B + \frac{1}{\tau D_{BC}} + \frac{1}{D_B}\right\}\mathbf{N}_B + \left\{\frac{(M_C/M_A)^{1/2}}{\tau D_{AB}} - \frac{1}{\tau D_{BC}}\right\}X_B\mathbf{N}_C = -\nabla c_B \tag{20a}$$

$$\left\{\frac{(M_B/M_A)^{1/2}}{\tau D_{AC}} - \frac{1}{\tau D_{BC}}\right\}X_C\mathbf{N}_B + \left\{\left(\frac{(M_C/M_A)^{1/2}}{\tau D_{AC}} - \frac{1}{\tau D_{BC}}\right)X_C + \left(\frac{1}{\tau D_{AC}} - \frac{1}{\tau D_{BC}}\right)X_A + \frac{1}{\tau D_{BC}} + \frac{1}{D_C}\right\}\mathbf{N}_C = -\nabla c_C \tag{20b}$$

Utilizing GFEM for the discretization, the approximate equations substituted for Eq. (20) at each nodal point become:

$$\sum_{j=1}^{np}\int_V \left\{\left(\frac{(M_B/M_A)^{1/2}}{\tau D_{AB}} - \frac{1}{\tau D_{BC}}\right)\bar{X}_B^{t+\Delta t,\,m} + \left(\frac{1}{\tau D_{AB}} - \frac{1}{\tau D_{BC}}\right)\bar{X}_A^{t+\Delta t,\,m} + \frac{1}{\tau D_{BC}} + \frac{1}{D_B}\right\}\Phi_i\Phi_j dV\mathbf{N}_{Bj}^{t+\Delta t,\,m+1} + \sum_{j=1}^{np}\int_V \left\{\frac{(M_C/M_A)^{1/2}}{\tau D_{AB}} - \frac{1}{\tau D_{BC}}\right\}\bar{X}_B^{t+\Delta t,\,m}\Phi_i\Phi_j dV\mathbf{N}_{Cj}^{t+\Delta t,\,m+1} = -\sum_{j=1}^{np}\int_V \Phi_i\nabla\Phi_j dV c_{Bj}^{t+\Delta t,\,m} \quad (i = 1 \sim np) \tag{21a}$$

$$\sum_{j=1}^{np}\int_V \left\{\frac{(M_B/M_A)^{1/2}}{\tau D_{AC}} - \frac{1}{\tau D_{BC}}\right\}\bar{X}_C^{t+\Delta t,\,m}\Phi_i\Phi_j dV\mathbf{N}_{Bj}^{t+\Delta t,\,m+1} + \sum_{j=1}^{np}\int_V \left\{\left(\frac{(M_B/M_A)^{1/2}}{\tau D_{AC}} - \frac{1}{\tau D_{BC}}\right)\bar{X}_C^{t+\Delta t,\,m} + \left(\frac{1}{\tau D_{AC}} - \frac{1}{\tau D_{BC}}\right)\bar{X}_B^{t+\Delta t,\,m} + \frac{1}{\tau D_{BC}} + \frac{1}{D_C}\right\}\Phi_i\Phi_j dV\mathbf{N}_{Cj}^{t+\Delta t,\,m+1} = -\sum_{j=1}^{np}\int_V \Phi_i\nabla\Phi_j dV c_{Cj}^{t+\Delta t,\,m} \quad (i = 1 \sim np) \tag{21b}$$

$\mathbf{N}_B$ and $\mathbf{N}_C$ can be given by the above-mentioned Eq. (21) from c_A, c_B, X_A, X_B and X_C which have been calculated on the previous Picard iteration step. On the other hand $\mathbf{N}_A$ can be calculated by Eq. (12) for Graham's law. The terms $\mathbf{N}_A$, $\mathbf{N}_B$, and $\mathbf{N}_C$ given by Eqs. (12) and (21) are substituted into Eq. (17), and c_A, c_B, and c_C on the latest Picard iteration step are calculated by Eq. (17). This numerical model is called the DG model hereafter.

Figure 4 shows a calculation flowchart for this numerical model. As presented in Fig. 4, molar fractions of each component are calculated from the initial concentrations of each component. Then the initial molar fluxes $\mathbf{N}_B$ and $\mathbf{N}_C$ are obtained based on the initial molar fractions by Eq. (21), and the initial $\mathbf{N}_A$ is calculated from $\mathbf{N}_B$ and $\mathbf{N}_C$ by Eq. (12). The values of $\mathbf{N}_A$, $\mathbf{N}_B$, and $\mathbf{N}_C$ given here are utilized to calculate c_A, c_B and c_C by Eq. (17) on the next Picard iteration step. $\mathbf{N}_A$, $\mathbf{N}_B$, and $\mathbf{N}_C$ are then updated by calculating from the new c_A, c_B and c_C values. The final values for c_A, c_B and c_C are determined when these concentrations converge to within a pre-set tolerance, and the simulation can be advanced to next time step. However the simulation is interrupted when c_A, c_B and c_C do not converge within the desired tolerance. The simulation is complete when the elapsed time in the simulation is equal to the specified maximum time.

VALUATION OF THE DEVELOPED NUMERICAL MODEL FOR THE MULTI-COMPONENT GAS SYSTEM IN GAS PHASE OF SOIL

In this section we illustrate differences between the numerical model developed in this study (the DG Model) and the numerical model with a diffusion coefficient calculated by Eq. (2) which can be used when the concentrations of components diffusing into gas phase of soil are very low. It has been described for the binary gas system in this study that a difference between molecular weights of components influences the diffusion in multi-component gas system, and that the diffusion coefficient of Eq. (2) derived from the dusty gas model could only be applied under restricted conditions, i.e., when the gas concentration is very low. However, Eq. (2) is very convenient for simulation of multi-component gas systems because the constituted equations are simpler and the

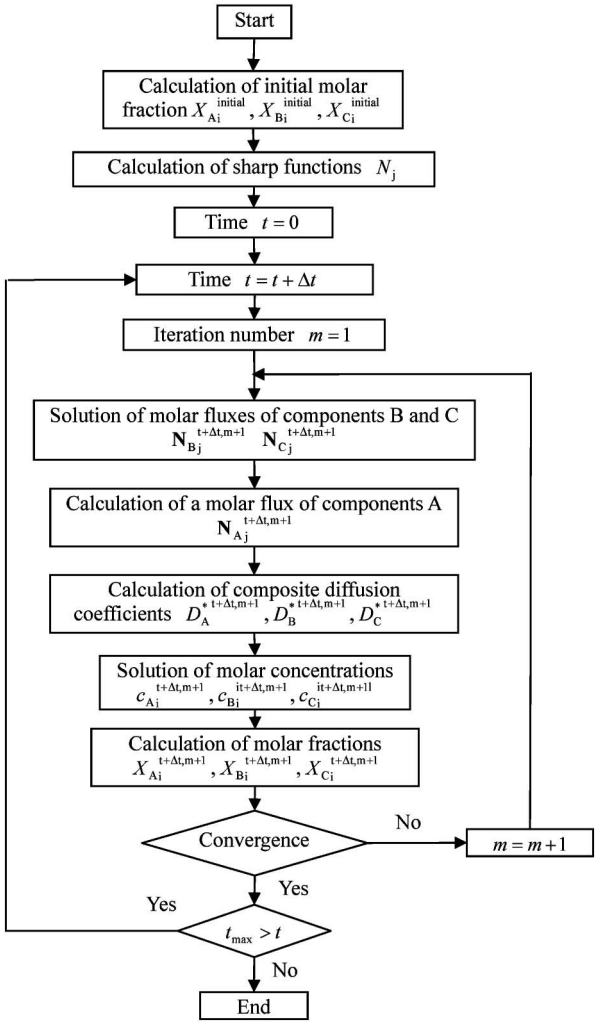

Fig. 4. The flowchart of the numerical simulation developed from the dusty gas model in this study for mass transfer of multiple components in the gas phase of soil

effort of computation can be decreased. The concentration at which Eq. (2) can be applied for multi-component gas systems can be decided by a comparison between the concentrations of components calculated by use of the DG model and the concentration given by Eq. (2), and it shall be verified that the DG model developed in this study is useful for multi-component gases in the gas phase of soil.

The constituted equations with diffusion coefficient calculated by Eq. (2) can be obtained from the conservative law and Fick's law. These constituted equations were already formulated by means of GFEM to compute the concentration of components in the soil gas phase. This numerical model is called modified Fick's law model (the MF model) thereafter.

The Case of Gas with Lower Molecular Weight than the Surrounding Gases

A simulation of methane diffusing into a region full of oxygen and nitrogen was carried out in this study because it illustrates the difference between distributions of concentrations given by means of the DG model and those given by means of the MF model. One dimensional elements were employed for both numerical models. The analytical domain specified over $0\,m \leq X \leq 10\,m$, and elements with nodal spacing of 0.05 m were used for both numerical models. The initial concentrations were: oxygen, 8.3 mol/m^3; nitrogen, 33.3 mol/m^3; and methane 0 mol/m^3 in $0 < X \leq 10$ m, except for $X = 0$ m as an initial condition. The total concentration was 41.6 mol/m^3 in $0\,m \leq X \leq 10\,m$.

Table 3. Parameters for simulations of multi-component gas systems if the molecular weight of gas diffusing into an analytical domain is lighter than that of other gas

Parameter	Value and/or Units
Tortuosity, τ	0.4
Component A Oxygen Molecular weight, M_A	32.00 g/mol
Component B Nitrogen Molecular weight, M_B	28.01 g/mol
Component C Methane Molecular weight, M_C	16.04 g/mol
Molecular diffusion coefficient between oxygen and nitrogen, D_{AB}	2.08×10^{-1} cm^2/s
Molecular diffusion coefficient between oxygen and methane, D_{AB}	2.27×10^{-1} cm^2/s
Molecular diffusion coefficient between nitrogen and methane, D_{BC}	2.13×10^{-1} cm^2/s

Methane molar fractions of 0.05, 0.10, 0.20 or 0.50 were specified at $X = 0$ m during the simulations. The concentrations of oxygen, nitrogen, and methane were specified to be 8.3, 31.22, and 2.08 mol/m^3 respectively when the molar fraction of methane was 0.05; 8.3, 29.14, and 4.16 mol/m^3 respectively when methane was set to 0.10; 8.3, 24.98, and 8.32 mol/m^3 respectively when 0.20; and 8.3, 12.54, and 20.8 mol/m^3 respectively when 0.50. On the other hand the molar fluxes of each component at 10 m were specified to be zero during the simulation, thus ensuring that no component was injected into the analytical domain or discharged from the analytical domain on the boundary located at 10 m.

Table 3 indicates the physical and chemical parameters used for simulations in the present study. Diffusion coefficients of each component are similar, however the molecular weight of methane is approximately half that of oxygen or nitrogen as shown in Table 3.

Figure 5 shows the concentration distributions of oxygen, nitrogen, and methane at an elapsed time of 8000 seconds when the molar fraction of methane is 0.05 at $X = 0$ m. As shown in Fig. 5, no difference can be distinguished between the distributions of the methane concentrations given by means of the DG model and that given by the MF model, and it can be seen that both concentrations are similar. On the other hand the concentration of oxygen given by means of the DG model is 1.4 mol/m^3 smaller than that given by the MF model at 10 m, and inversely the concentration given by the DG model for nitrogen is 1.4 mol/m^3 larger than that given by means of the MF model. These tendencies of migrations with oxygen and nitrogen can be confirmed in Fig. 6 which illustrates the distributions of the concentrations of oxygen and nitrogen when the molar fraction of methane is 0.10 at $X = 0$ m, but the difference between the concentrations

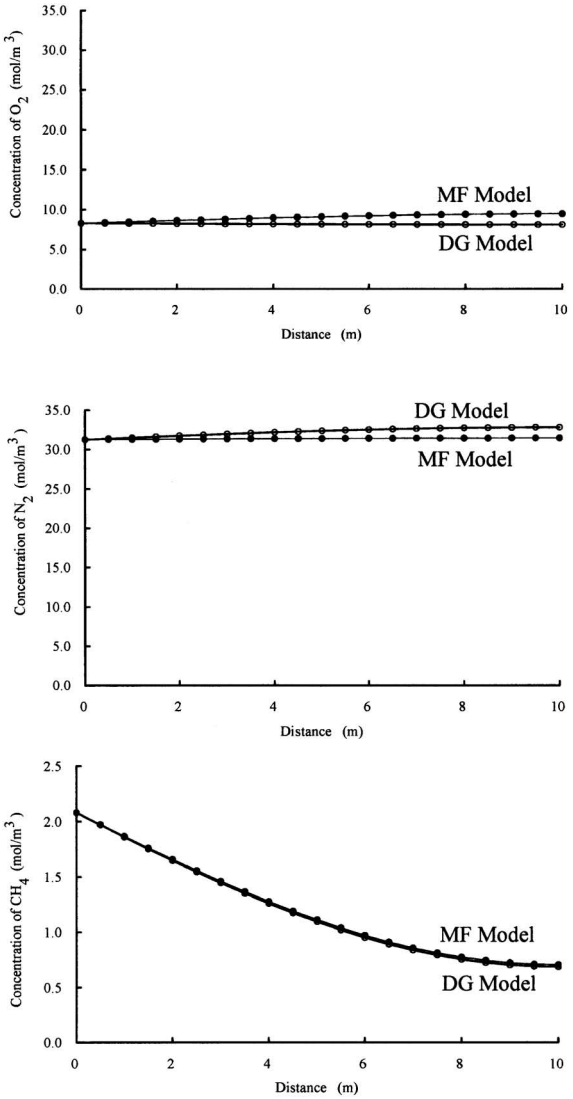

Fig. 5. Distributions of concentrations of oxygen, nitrogen, and methane after 8000 seconds of simulation for a molar fraction of methane of 0.05. White circles represent concentrations given by DG model, and filled circles the case of MF model

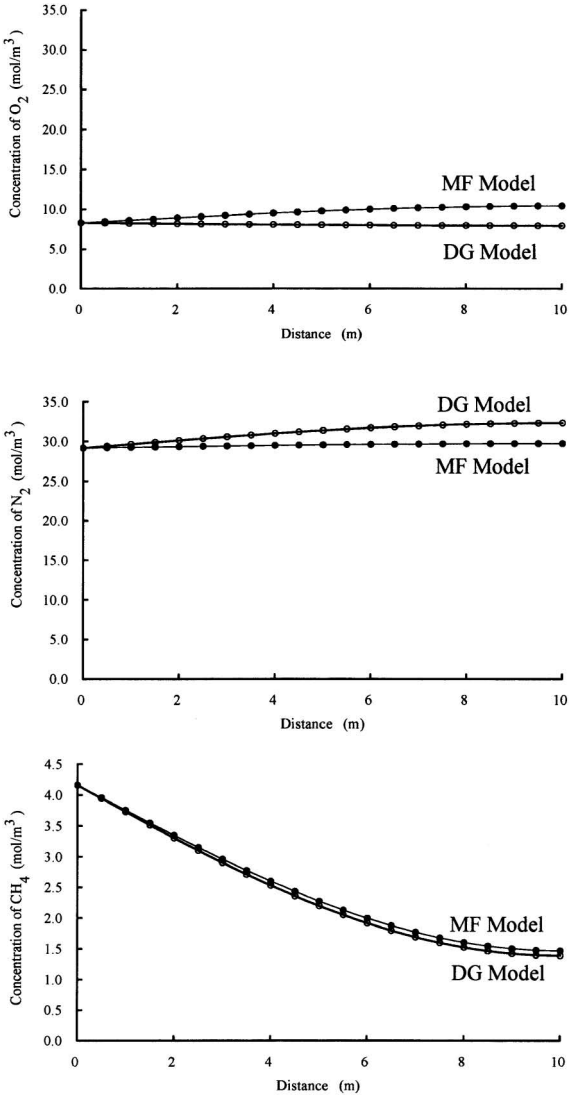

Fig. 6. Distributions of concentrations of oxygen, nitrogen, and methane after 8000 seconds of simulation for a molar fraction of methane of 0.10. White circles represent concentrations given by DG model, and filled circles the case of MF model

given by the two models for methane is not distinct because this difference becomes 0.08 mol/m^3 at $X = 10$ m.

Figure 7 shows distributions of each concentration when the molar fraction of methane is set to 0.20 at $X = 0$ m, and Fig. 8 shows concentration distributions for a methane molar fraction of 0.50. As shown in Fig. 7, the differences between the concentrations given by the DG and MF models are more obvious than those shown in Fig. 6, and the difference between concentrations of methane given by each numerical model becomes 0.35 mol/m^3. A larger difference in predicted methane concentrations appeared for a molar methane fraction of 0.5, as seen in Fig. 8. The results shown in Figs. 7 and 8 confirm that the differences between the concentrations of oxygen and nitrogen given by the DG model and MF model increase with the molar fraction of methane at $X = 0$ m.

Therefore the diffusion coefficient calculated by Eq. (2) can be used for the multi-component gas system simulation with a molar fraction of methane of 0.10 or less, if the diffusing component has a lighter molecular weight than those of the components filling the domain. The DG model composed in this study must be used to simulate the migrations of each component in a multi-component gas system if the molar fraction of methane exceeds 0.10. However, regarding the migrations of components which initially exist in the domain, the distinct difference between the results given by the DG and MF models is present for the entire range of methane molar fraction.

The Case of Gas with Higher Molecular Weight than the Surrounding Gases

The DG and MF models have been evaluated in the previous section for the condition of a lower molecular weight component diffusing through a domain of higher molecular weight gases. Applicability of these models will be examined for the condition of a diffusing component

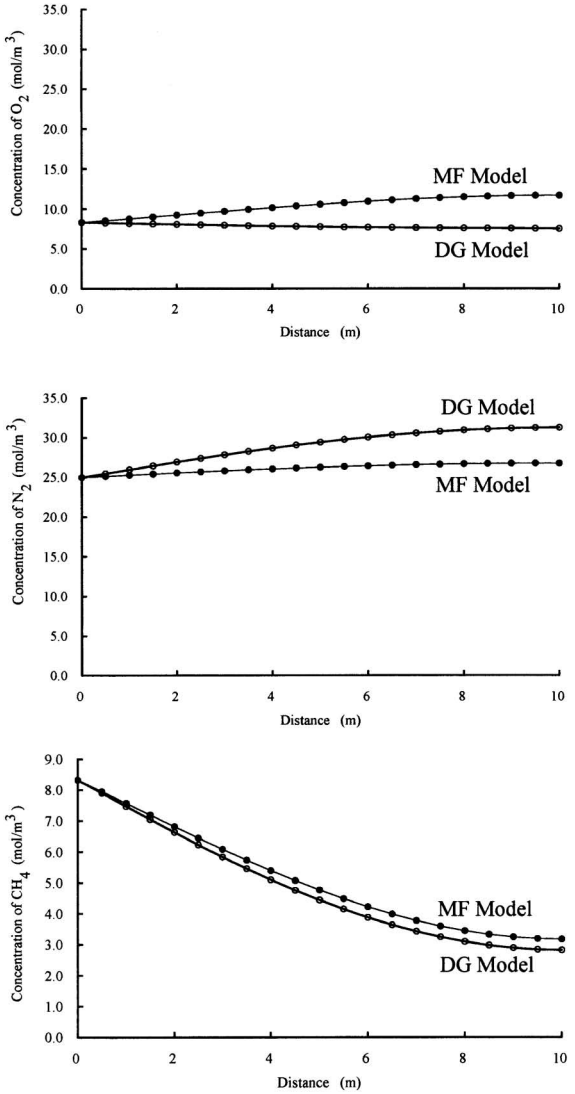

Fig. 7. Distributions of concentrations of oxygen, nitrogen, and methane after 8000 seconds of simulation for a molar fraction of methane of 0.20. White circles represent concentrations given by DG model, and filled circles the case of MF model

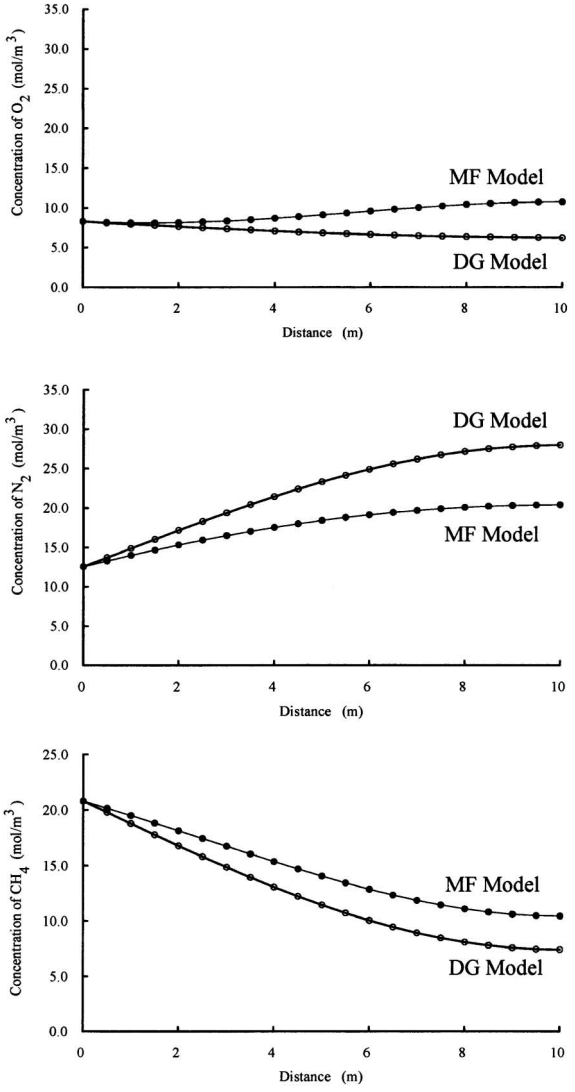

Fig. 8. Distributions of concentrations of oxygen, nitrogen, and methane after 8000 seconds of simulation for a molar fraction of methane of 0.50. White circles represent concentrations given by DG model, and filled circles the case of MF model

with higher molecular weight than the background gases. The extent of the analytical domain, the discretization scheme, and the initial and boundary conditions are equivalent in the case of methane.

Table 4 indicates the physical and chemical parameters used for the simulations presented here, with TCE as the diffusing gas. The molecular weight of TCE is approximately four times that of oxygen and nitrogen as shown in Table 4, and the diffusion coefficient between TCE and oxygen or nitrogen is approximately 1/3 that between oxygen and nitrogen.

Figure 9 shows distributions of oxygen, nitrogen, and TCE concentrations when the mole fraction of TCE is 0.05 at $X=0$ m after an elapsed simulation time of 30000 seconds. Figure 10 shows these concentrations for an initial TCE fraction of 0.10, Fig. 11 for 0.20, and Fig. 12 for 0.50.

It can be seen in Fig. 9 that the concentrations given by the DG model for oxygen and nitrogen are similar to those given by the MF model. However, the differences in predicted TCE concentrations given by the DG model and the MF model are slightly greater than those predicted in the case of methane. The concentration given by the

Table 4. Parameters for simulations of multi-component gas systems if the molecular weight of the gas diffusing into an analytical domain is heavier than that of other gas

Parameter	Value and/or Units
Tortuosity, τ	0.4
Component A Oxygen Molecular weight, M_A	32.00 g/mol
Component B Nitrogen Molecular weight, M_B	28.01 g/mol
Component C TCE Molecular weight, M_C	131.4 g/mol
Molecular diffusion coefficient between oxygen and nitrogen, D_{AB}	2.08×10^{-1} cm^2/s
Molecular diffusion coefficient between oxygen and TCE, D_{AB}	7.60×10^{-2} cm^2/s
Molecular diffusion coefficient between nitrogen and TCE, D_{BC}	7.60×10^{-2} cm^2/s

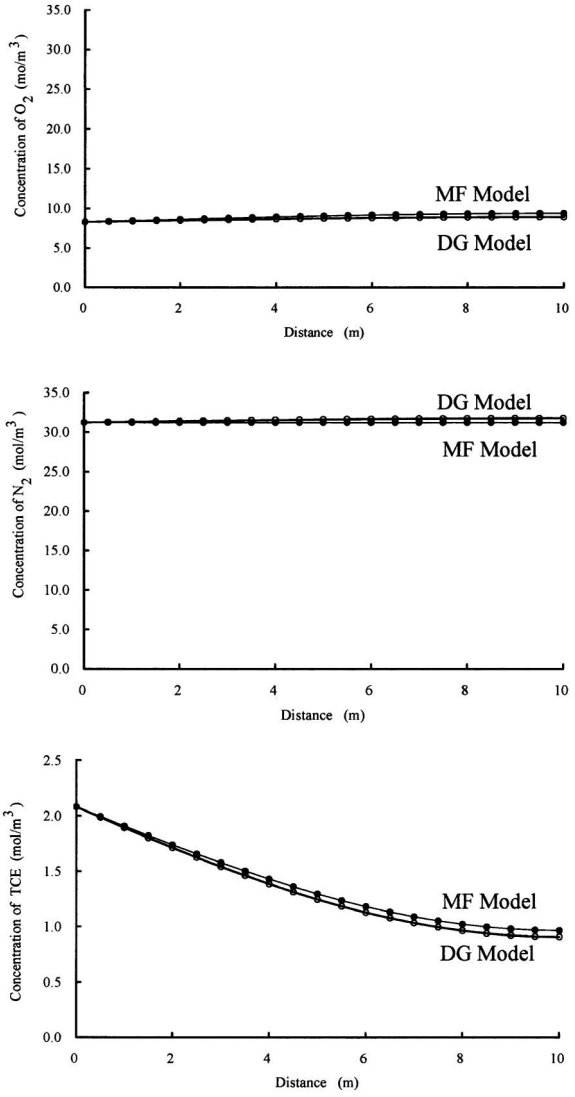

Fig. 9. Distributions of concentrations of oxygen, nitrogen, and trichloroethylene at 30000 seconds for a molar fraction of trichloroethylene of 0.05. White circles represent concentrations given by DG model, and filled circles the case of MF mode

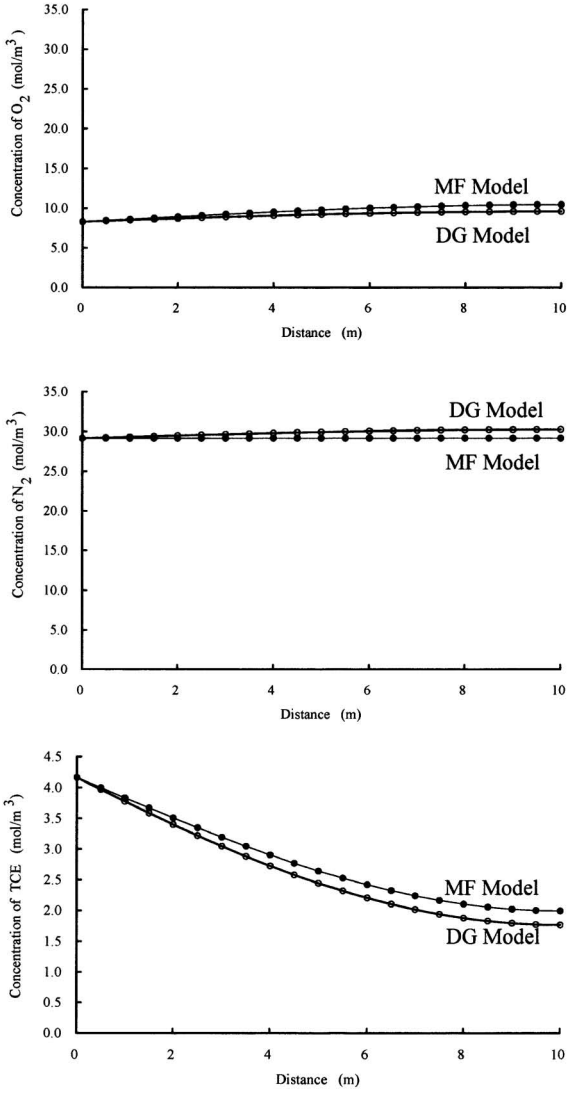

Fig. 10. Distributions of concentrations of oxygen, nitrogen, and trichloroethylene at 30000 seconds for a molar fraction of trichloroethylene of 0.10. White circles represent concentrations given by DG model, and filled circles the case of MF mode

DG model for TCE is 0.058 mol/m^3 lower than that given by the MF model.

The concentration of TCE given by the DG model is 1.76 mol/m^3 at $X=10$ m as shown in Fig. 10, while that given by the MF model is 1.99 mol/m^3 at $X=10$ m, a difference of 0.23 mol/m^3, just as shown in Fig. 10. The difference between both concentrations is 5.5 percent of the boundary value concentration of 4.16 mol/m^3 specified and $X=0$ m. The oxygen and nitrogen differences of the concentrations given by the DG model are indicated in Fig. 10. The concentration of oxygen given by the DG model is slightly lower than that given by the MF model, while the DG model predicts a higher nitrogen concentration than the MF model, as shown in Fig. 10. These differences in regard to oxygen, nitrogen, and TCE become greater as the concentration of TCE at $X=0$ m increases, as can be seen by comparing Figs. 10 and 11. When the molar fraction of TCE is 0.50 at $X=0$ m, the difference between the TCE concentrations given by the DG model and MF model is 6.37 mol/m^3, the difference between the concentrations for oxygen is 3.3 mol/m^3, and the difference between the concentrations for nitrogen is 3.1 mol/m^3, as shown in Fig. 12.

Therefore the concentration calculated for the component diffusing into the domain is different depending on the type of numerical method used, even if the molar fraction of TCE is very low (0.05) at $X=0$ m, when the molecular weight of the diffusing component is higher than that of the components which initially exist in the domain. The concentrations simulated by the DG and MF models for oxygen and nitrogen are similar when the molar fraction of TCE is 0.05 at $X=0$ m; however differences between the concentrations simulated by the two models for TCE, oxygen, and nitrogen at $X=10$ m increase with increasing molar fraction of TCE at the inlet of the diffusing component.

Consequently, the diffusion coefficient calculated by Eq. (2) for a diffusing component of higher molecular

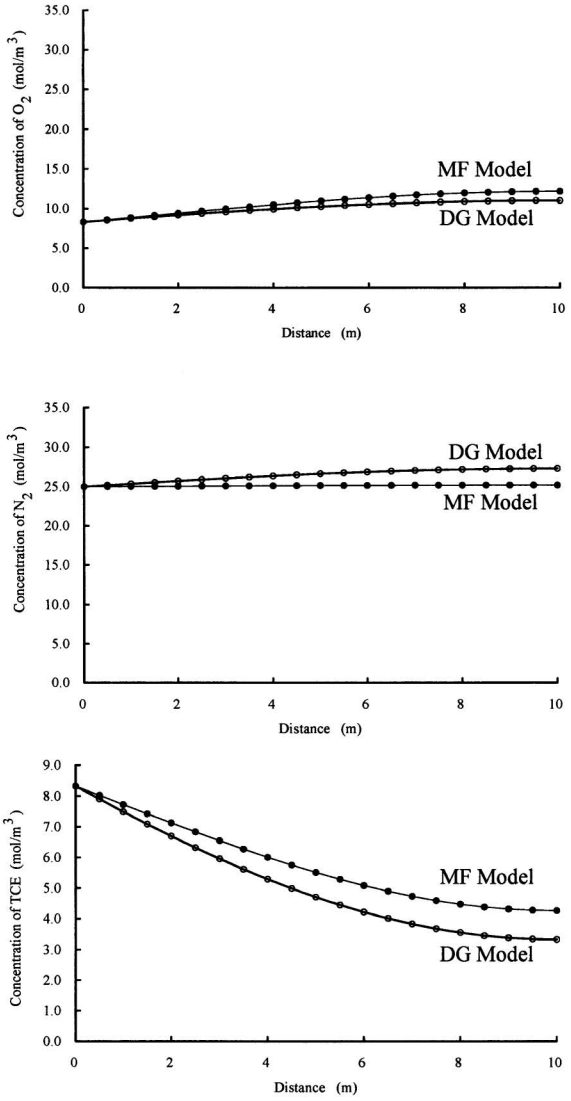

Fig. 11. Distributions of concentrations of oxygen, nitrogen, and trichloroethylene at 30000 seconds for a molar fraction of trichloroethylene of 0.2. White circles represent concentrations given by DG model, and filled circles the case of MF mode

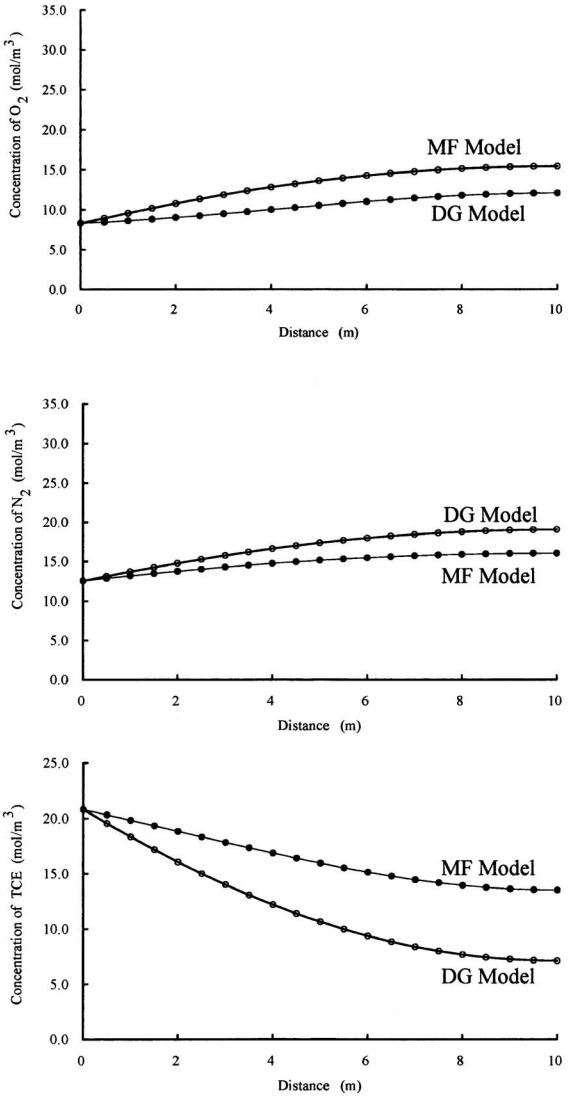

Fig. 12. Distributions of concentrations of oxygen, nitrogen, and trichloroethylene at 30000 seconds for a molar fraction of trichloroethylene of 0.5. White circles represent concentrations given by DG model, and filled circles the case of MF mode

weight than those of the surrounding components must not be used in the case that the concentration of the diffusing component is very low. The DG model developed in this study may be used in this case.

CONCLUSION

By comparison between a Fick's law of diffusion coefficient for a binary gas system and a diffusion coefficient derived by means of the dusty gas model and Graham's law for the binary gas system with a very dilute diffusing gas, it became obvious that the diffusion coefficient given by means of the dusty gas model and Graham's law could be used only if the concentration of the diffusing gas is considerably dilute. Furthermore, it was found in this study that the difference in component molecular weights influences the diffusion coefficient in a binary gas system when the diffusion coefficient is given by means of the dusty gas model and Graham's law, as compared with the diffusion coefficient in Fick's law. The concentration of an actual gas phase pollutant in the soil is likely to extend over a large range, since the gas phase molar fraction will be high in the vicinity of the volatile liquid pollution source and will drop off with distance from the liquid source. Consequently it was illustrated in this study that the dusty gas model must be applied for multi-component gas systems in the gas phase of soil.

The numerical model to simulate mass transfer of multiple components in the soil gas phase has been developed by means of FEM from the duty gas model for a multi-components gas system. The diffusion coefficient calculated by Eq. (2) which is applied for gas phase diffusion of a component with very low concentration has often been used instead of the diffusion coefficient in Fick's law. Complexity of the calculation can be avoided by employing Eq. (2), reducing the effort of computation.

However, it was found in this investigation that Eq. (2) could be applied for multi-component gas systems only for concentrations of the diffusing component that did not exceed 0.10, even in the case of methane which is lighter than the molecular weights of the surrounding components. It was also found that Eq. (2) could not be employed to simulate mass transfer for components which were heavier than the molecular weights of the surrounding components in a multi-component gas system, even if the molar fraction of this component was 0.05 at a boundary of the domain. The distributions of the concentrations simulated by the DG model were different than those simulated by the MF model, and it has been confirmed that the DG model developed in this study must be applied for modeling multi-component diffusion in the soil gas phase.

Only diffusion has been estimated in this study; a complete model must also include advection. It may be possible to introduce the dusty gas model into the diffusion-advection or dispersion-advection equations by means of the numerical model developed in this study.

NOTATION

c total concentration [mol/L^3]
c_i molar concentration [mol/L^3] of component i
D_i Knudsen coefficient [L^2/T]
D_{ij} binary molecular diffusion coefficient [L^2/T] between component i and component j
D_{im} molecular diffusion coefficient [L^2/T] in the multi-component gas system

$$D_A^* = 1\Big/\left(\frac{X_B}{\tau D_{AB}} + \frac{X_C}{\tau D_{AC}} + \frac{1}{D_A}\right)$$

$$D_B^* = 1\Big/\left(\frac{X_A}{\tau D_{AB}} + \frac{X_C}{\tau D_{BC}} + \frac{1}{D_B}\right)$$

$$D_C^* = 1\Big/\left(\frac{X_A}{\tau D_{AC}} + \frac{X_B}{\tau D_{BC}} + \frac{1}{D_C}\right)$$

$$D_{AB}^* = 1\Big/\left(\frac{X_A}{\tau D_{AB}}\left(\frac{M_A}{M_B}\right)^{1/2} + \frac{X_B}{\tau D_{AB}} + \frac{1}{D_A}\right)$$

$$D_{BA}^* = 1\Big/\left(\frac{X_B}{\tau D_{AB}}\left(\frac{M_B}{M_A}\right)^{1/2} + \frac{X_A}{\tau D_{AB}} + \frac{1}{D_B}\right)$$

$\bar{D}_A^*$ average of the respective values of D_A^* within each element
$\bar{D}_B^*$ average of the respective values of D_B^* within each element
$\bar{D}_C^*$ average of the respective values of D_C^* within each element
M_i molecular weights [M/mol] of component i
m iteration number of the Picard iteration method
Φ_i basic function at node i
$\mathbf{N}_i$ molar flux [mol/L^{2}T] of component i
$\mathbf{N}^D$ molar diffusion gas flux [mol/L^{2}T]
$\mathbf{N}^N$ nonequimolar diffusion gas flux [mol/L^{2}T]
$\mathbf{N}^T$ total molar diffusion flux [mol/L^{2}T]
$\mathbf{n}$ normal vector to boundary Ω
n the number of nodes
np the number of components
$\mathbf{q}_i$ molar fluxes [mol/L^{2}T] of components i at the boundary
t elapsed time
V whole volume [L^3]
X_i molar fraction [dimensionless] of component i
$\bar{X}_j$ average of the respective values of X_i within each element
Δt increment of elapsed time
θ_g gas-filled porosity
$\bar{\theta}_g$ average of the respective values of θ_g within each element
τ tortuosity [dimensionless]
Ω boundary of an analytical domain

REFERENCES

1) Abriola, L. and Pinder, G. F. (1985): A multiphase approach to the modeling of porous media contamination by organic compounds 1 Equation development, *Water Resources Research*, **21**(1), 11–18.
2) Abriola, L. and Pinder, G. F. (1985): A multiphase approach to the modeling of porous media contamination by organic compounds 2 Numerical simulation, *Water Resources Research*, **21**(1), 19–26.
3) Baehr, A. L. and Corapciglu, M. Y. (1987): A compositional multiphase model for groundwater contamination by petroleum products 2 Numerical solution, *Water Resources Research*, **23**(1), 2001–2132.
4) Baehr, A. L. and Bruell, C. J. (1990): Application of the Stefan-Maxwell equations to determine limitations of Fick's low when modeling organic vapor transport in sand columns, *Water Resources Research*, **26**(6), 1155–1163.
5) Celia, M. and Bouloutas, E. T. (1990): A General mass-conservative numerical solution for the unsaturated flow equation, *Water Resources Research*, **26**(7), 1483–1496.
6) Corapciglu, M. Y. and Baehr, A. L. (1987): A compositional multiphase model for groundwater contamination by petroleum products 1 Theoretical considerations, *Water Resources Research*, **23**(1), 191–200.
7) Costanza-Robison, M. S. and Brusseau, M. L. (2002): Gas phase advection and dispersion in unsaturated porous media, *Water Resources Research*, **38**(4), 7–1–7–10.
8) Cunnigham, R. E. and Williams, R. J. J. (1980): *Diffusion Gases and Porous Media*, Plenum Press, 1–80.
9) Curtiss, C. F. and Hirschfelder, J. O. (1949): Transport properties of multicomponent gas mixtures, *Journal of Chemical Physics*, **17**, 550–555.
10) Fischer, U., Schulin, R., Keller, M. and Stauffer, F. (1996): Experimental and numerical investigation of soil vapor extraction, *Water Resources Research*, **32**(12), 3413–3427.
11) Hoeg, S., Scholer, H. F. and Warnatz, J. (2004): Assessment of interfacial mass transfer in water-unsaturated soils during vapor extraction, *Journal of Contaminant Hydrology*, **74**, 163–193.
12) Jellali, S., Benremita, H., Muntzer, P., Razakarisoa, O. and Schader, G. (2003): A large-scale experiment on mass transfer of trichloroethylene from the unsaturated zone of a sandy aquifer to its interfaces, *Journal of Contaminant Hydrology*, **60**, 31–53.
13) Klinkenberge, L. J. (1941): The permeability of porous media to liquids and gases, *Drilling and Production Practice*, 200–213.
14) Knesfsey, T. J. and Hunt, J. R. (2004): Non-aqueous phase liquid spreading during soil vapor extraction, *Journal of Contaminant Hydrology*, **68**, 143–164.
15) Lenhard, R. J., Oostrom, M., Simmons, C. S. and White, M. D. (1995): Investigation of density-dependent gas advection of trichloroethylene: Experiment and a model validation exercise,

Journal Contaminant Hydrology, **19**, 47–67.
16) Mason, E. A. (1967): Flow and diffusion of gases in porous media, *Journal of Chemical Physics*, **46**, 3199–3216.
17) Mason, E. A. and Malinauskas, A. P. (1983): *Gas Transport in Porous Media the Dusty Gas Model*, Elsevier, 30–49.
18) Massmann, J. and Farrier, D. F. (1992): Effects of atmospheric pressures on gas transport in the vapor zone, *Water Resources Research*, **28**(3), 777–791.
19) Mendoza, A. and Frind, E. O. (1990): Advective-Dispersion transport of dense organic vapor in unsaturated zone 1. Model development, *Water Resources Research*, **26**(3), 379–387.
20) Mendoza, A. and Frind, E. O. (1990): Advective-Dispersion transport of dense organic vapor in unsaturated zone 2. Sensitivity analysis, *Water Resources Research*, **26**(3), 388–398.
21) Millingtion, R. J. (1959): Gas diffusion in porous media, *Science*, **130**, 100–102.
22) Milly, P. C. D. (1985): A mass-conservative procedure for time-stepping in models of unsaturated flow, *Advance Water Resources*, **23**(8), 32–36.
23) Poling, B. E., Prausnitz, J. M. and O'Connell, J. P. (2001): The properties of gases and liquids, McGraw-Hill, 11.19–11.20.
24) Reinecke, S. A. and Sleep, B. E. (2002): Knudsen diffusion, gas permeability, and water content in an unconsolidated porous medium, *Water Resource Research*, **38**(12), 16–1–16–15.
25) Shan, C., Falta, R. W. and Javandel, I. (1992): Analytical solution for steady state gas flow to a soil vapor extraction well, *Water Resources Research*, **28**, 1105–1120.
26) Sleep, B. E. and Sykes, J. F. (1989): Modeling the transport of volatile organics in variably saturated media, *Water Resources Research*, **25**(1), 81–92.
27) Sleep, B. E. and Sykes, J. F. (1993): Compositional simulation of groundwater contamination by organic compounds 1. Model development and verification, *Water Resources Research*, **29**(6), 1697–1708.
28) Sleep, B. E. and Sykes, J. F. (1993): Compositional simulation of groundwater contamination by organic compounds 2. Model applications, *Water Resources Research*, **29**(6), 1709–1718.
29) Thorstenson, D. C. and Pollock, D. W. (1989): Gas transport in unsaturated zones: Multicomponent systems and the adequacy of Fick's Laws, *Water Resources Research*, **25**(3), 477–507.